

Imaging multipole magnetic susceptibility anisotropy in vivo

Chunlei Liu¹ and Wei Li¹

¹Brain Imaging and Analysis Center, Duke University, Durham, NC, United States

PURPOSE: Current methods for imaging magnetic susceptibility rely solely on the mean phase of a voxel (1, 2). The spatial heterogeneity of magnetic fields within a voxel, however, is lost during the ensemble averaging. If the field distribution can be recovered, it may allow us to infer the underlying tissue microstructure. The purpose of the study was to test a novel method to measure such higher-order frequency variations *in vivo* on human brains. The method requires only a single volume of gradient echo images. It utilized a multipole analysis of the MRI signal in a sub-voxel Fourier spectral space termed “**p**-space” for short. By sampling the **p**-space with shifted image reconstruction, we were able to measure a set of dipole and quadrupole susceptibility tensors. We developed an algorithm to estimate these tensors from data acquired with multiple-channel receiver coils. We showed that multipole tensors offer a set of new contrast for *in vivo* brain imaging. The eigenvectors of these tensors may provide new insights into tissue microstructures. Because it does not require any rotations, this **p**-space method of susceptibility tensor imaging (STI) may potentially enable routine imaging of susceptibility anisotropy, overcoming the challenges encountered in the original STI (3) that requires rotations.

METHODS: The distribution of magnetic field within a voxel can be analyzed in the Fourier domain (the **p**-space). One way to sample the **p**-space is by applying an external magnetic field gradient vector which will modulate the resonance frequency of the spins within the voxel. In the presence of a pulsed field-gradient **G**, the voxel-averaged MRI signal $s(\mathbf{r})$ at time t , ignoring T_2 -relaxation, can be shown to be described by Eq. [1]. In a second-order multipole expansion, $\Phi(\mathbf{r}, \mathbf{p})$ can be written as in Eq. [2]. The first term is the mean phase. The second term is a dipole moment in which χ_d is a rank-2 dipole susceptibility tensor and $\hat{\mathbf{p}}$ is the unit directional vector. The third term is a quadrupole moment expressed in terms of a rank-2 quadrupole susceptibility tensor χ_q . More specifically, Φ_0 is the phase when no gradient is applied and it is related to the image-space dipole susceptibility tensor (rank 2) $\chi(\mathbf{r})$ following (3). The magnitude can be expanded similarly. To reconstruct an image in the **p**-space, we simply shifted the raw **k**-space data with the desired **p**-vector. This strategy allowed the sampling of the **p**-space without applying physical gradients. By shifting the reconstruction window in various directions and with various distances, a series of images can be reconstructed (Fig. 1). For each shift in the **p**-space, a linear phase term was also introduced to the image as described in Eq. [1]. This linear phase was removed before calculating the phase spectrum (Fig. 1). All magnitude and phase images were normalized by their corresponding values at $p = 0$. This procedure is applied on a coil-by-coil basis. No phase unwrapping was necessary.

Healthy adult volunteers were scanned on a 3.0T GE MR750 scanner equipped with an 8-channel head coil. Images were acquired using a 16-echo 3D SPGR sequence with the following parameters: FOV = 192x192x120 mm³, matrix size = 192x192x120, BW = 62.5 kHz, flip angle = 20°, TE of the first echo = 4.0 ms, echo spacing = 2.3 ms and TR = 50.0 ms. Total scan time was 19.2 minutes.

RESULTS: In the white matter, the signal showed a strong dependence on the p -value while in the gray matter it stayed relatively constant (Fig. 2). For the dipole terms (2nd term of Eq. [2]), the inverse of the standard deviations (i.e. $1/\delta m_d$ and $1/\delta f_d$) showed a clear dependence on the orientation of the **p**-vector (Fig. 3a). When the axons were parallel to the **p**-vector, both $1/\delta m_d$ and $1/\delta f_d$ were the largest in the corresponding white matter regions such as the posterior corona radiata (pcr) at $\mathbf{p} = [1 \ 0 \ 0]$ and the splenium of the corpus callosum (scc) at $\mathbf{p} = [0 \ 1 \ 0]$ (Fig. 3a). In other words, when the axons were parallel to the **p**-vector, δm_d and δf_d were the smallest. Based on Eq. [2], we

computed the dipole susceptibility tensors (χ_d in Fig. 3c). The orientation of the minimal eigenvector was color-coded with red representing red-left, green representing anterior-posterior and blue representing superior-inferior (Fig. 3c). Finally, only the quadrupole term of the magnitude didn't show significant orientation dependence; however, it provided excellent tissue contrast that mimics T2-weighted images (Fig. 3b).

DISCUSSIONS AND CONCLUSIONS: A method was proposed and demonstrated to extract sub-voxel information of tissue magnetic response *in vivo*. This sub-voxel magnetic response was characterized by a set of magnetic multipoles which can be obtained by analyzing gradient-echo images in the **p**-space. An algorithm was developed to perform **p**-space analysis for gradient-echo images acquired with multiple coils. We have a number of unique findings: 1) multipole response of white matter exhibits strong dependence on p -value; 2) multipole response of white matter is anisotropic; 3) multipole tensors provide distinctive contrasts; 4) multipole tensors are indicative of tissue microstructure. Most importantly, this unique information can be obtained from a single volume of GRE images as apposed to the original STI which requires rotation of the brain or the magnetic field. While the feasibility of the original STI setup has been demonstrated *in vivo* on human brains (4), its routine application has so far been limited to imaging specimens *ex vivo*. The proposed **p**-space STI may overcome this limitation and potentially allow the imaging of tissue microstructure from a single GRE scan. The current work proposed and developed a practical method for imaging these anisotropic susceptibility tensors. A complete understanding of the relationship between these tensors, cellular organization and fiber orientations requires further investigation. Correlating the results with DTI (5) may provide additional insights. In the simple case of parallel axons, we identified the minor eigenvectors of three susceptibility tensors were aligned with the axons. The technique will benefit from the utilization of higher magnetic field and improved field shimming.

REFERENCES: 1. Haacke, E.M. et al, MRM 2004; 52:612-618. 2. Duyn, J.H. et al, PNAS 2007; 104:11796-11801. 3. Liu, C., MRM 2010; 63:1471-1477. 4. Li, W. et al, NeuroImage 2011; 59:2088-2097. 5. Bassler, P.J. et al, Biophys J. 1994; 66:259-267.

$$s(\mathbf{r}) = e^{-i2\pi\mathbf{p}\cdot\mathbf{r}} m(\mathbf{r}, \mathbf{p}) e^{-i\Phi(\mathbf{r}, \mathbf{p})} \quad [1]$$

$$\Phi(\mathbf{p}) = \Phi_0 + \gamma B_0 t \hat{\mathbf{p}}^T \chi_d \hat{\mathbf{p}} + \gamma B_0 t \hat{\mathbf{p}}^T \chi_q \hat{\mathbf{p}} p^2 \quad [2]$$

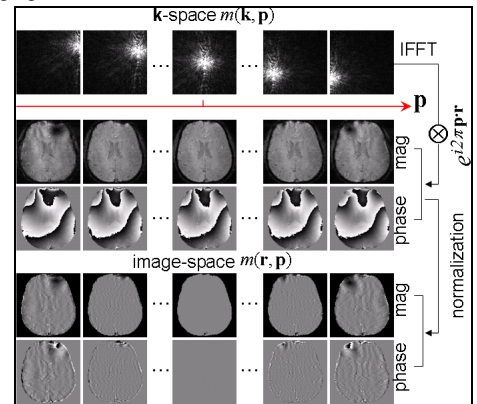


Figure 1. Methods for reconstructing images in the **p**-space. **k**-Space data were shifted in various directions. Magnitude and phase images were obtained as shown in the flow chart.

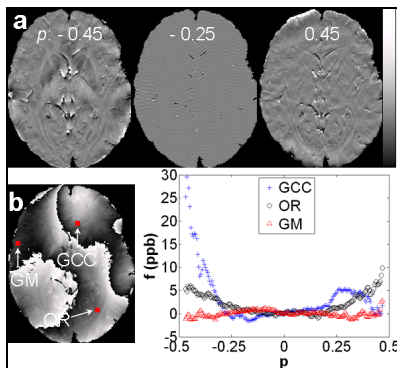


Figure 2. Signal behavior in the **p**-space. (a) Phase maps at three p -values along the p_y direction. (b) Plots of frequency shift as a function of p -value in the genu of corpus callosum (GCC), optical radiation (OR) and gray matter (GM).

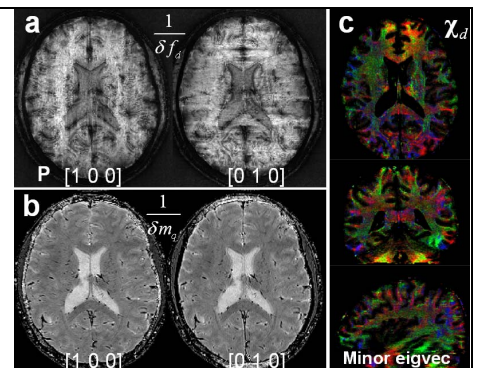


Figure 3. Examples of multipole susceptibility tensors reconstructed in the **p**-space. (a) Dipole frequency variations show strong orientation dependence. (b) Quadrupole magnitude variations do not show significant orientation dependence but offer great tissue contrast. (c) Orientation of eigenvectors.